Molecular Human Reproduction, Vol.21, No.11 pp. 832–843, 2015
Advanced Access publication on September 7, 2015 doi:10.1093/molehr/gav049

molecular human reproduction

ORIGINAL RESEARCH

Plasma membrane Ca^{2+}-ATPase 4: interaction with constitutive nitric oxide synthases in human sperm and prostasomes which carry Ca^{2+}/CaM-dependent serine kinase

Rachel E. Andrews, Deni S. Galileo, and Patricia A. Martin-DeLeon*

Department of Biological Sciences, University of Delaware, Newark, DE 17916, USA

*Correspondence address. E-mail: pdeleon@udel.edu

Submitted on December 17, 2014; resubmitted on August 21, 2015; accepted on August 31, 2015

ABSTRACT: Deletion of the gene encoding the widely conserved plasma membrane calcium ATPase 4 (PMCA4), a major Ca^{2+} efflux pump, leads to loss of sperm motility and male infertility in mice. PMCA4's partners in sperm and how its absence exerts its effect on fertility are unknown. We hypothesize that in sperm PMCA4 interacts with endothelial nitric oxide synthase (eNOS) and neuronal nitric oxide synthase (nNOS) which are rapidly activated by Ca^{2+}, and that these fertility-modulating proteins are present in prostasomes, which deliver them to sperm. We show that in human sperm PMCA4 is present on the acrosome, inner acrosomal membrane, posterior head, neck, midpiece and the proximal principal piece. PMCA4 localization showed inter- and intra-individual variation and was most abundant at the posterior head/neck junction, co-localizing with NOSs. Co-immunoprecipitations (Co-IP) revealed a close association of PMCA4 and the NOSs in Ca^{2+} ionophore-treated sperm but much less so in uncapacitated untreated sperm. Fluorescence resonance energy transfer (FRET) showed a similar Ca^{2+}-related association: PMCA4 and the NOSs are within 10 nm apart, and preferentially so in capacitated, compared with uncapacitated, sperm. FRET efficiencies varied, being significantly ($P < 0.001$) higher at high cytosolic Ca^{2+} concentration ($[Ca^{2+}]_c$) in capacitated sperm than at low $[Ca^{2+}]_c$ in uncapacitated sperm for the PMCA4-eNOS complex. These dynamic interactions were not seen for PMCA4-nNOS complexes, which had the highest FRET efficiencies. Further, along with Ca^{2+}/CaM-dependent serine kinase (CASK), PMCA4 and the NOSs are present in the seminal plasma, specifically in prostasomes where Co-IP showed complexes similar to those in sperm. Finally, flow cytometry demonstrated that following co-incubation of sperm and seminal plasma, PMCA4 and the NOSs can be delivered *in vitro* to sperm via prostasomes. Our findings indicate that PMCA4 interacts simultaneously with the NOSs preferentially at high $[Ca^{2+}]_c$ in sperm to down-regulate them, and thus prevent elevated levels of NO, known to induce asthenozoospermia via oxidative stress. Our studies point to the potential underlying cause of infertility in PMCA4's absence, and suggest that inactivating mutations of *PMCA4* could lead to asthenozoospermia and human infertility. Screening for these mutations may serve both diagnostic and therapeutic purposes.

Key words: calcium efflux / nitric oxide regulation / prostasomes / sperm motility / male infertility

Introduction

Calcium extrusion from the cytosol, like its influx, is essential for maintaining normal sperm motility and fertility, yet little is known of the mechanisms involved in human sperm. While mammalian sperm have specialized compartments, such as mitochondria, in which calcium can be sequestered when cytosolic levels are elevated, Ca^{2+} efflux into the extracellular space is dependent on two transporters: the sodium/calcium exchanger (NCX) and plasma membrane calcium ATPase 4 (PMCA4) (Wennemuth *et al.*, 2003). The highly conserved PMCA4 has been shown to be the major Ca^{2+} efflux pump in the murine system, being far more effective than both the NCX and the mitochondrial calcium uniporter combined in Ca^{2+} clearance from the cytosol (Wennemuth *et al.*, 2003).

PMCA4 which is ubiquitously expressed has two isoforms, 4a and 4b, with the latter maintaining a steep Ca^{2+} gradient between the intracellular and the extracellular space and also functioning as a modulator of signal transduction pathways (DeMarco and Strehler, 2001; Di Leva *et al.*, 2008), while 4a is faster (Caride *et al.*, 2007). When the murine gene (*Pmca4*) is deleted, intracellular Ca^{2+} is significantly elevated, accompanied by Ca^{2+} overload in the mitochondria, resulting in the loss of progressive and hyperactivated sperm motility which subsequently

© The Author 2015. Published by Oxford University Press on behalf of the European Society of Human Reproduction and Embryology. All rights reserved.
For Permissions, please email: journals.permissions@oup.com

Downloaded from https://academic.oup.com/molehr/article/21/11/832/2459813 by guest on 24 April 2024

leads to male infertility (Okunade *et al.*, 2004; Schuh *et al.*, 2004). Similarly, a significant decrease in progressive sperm motility and a more severe reduction in hyperactivated motility (Shao *et al.*, 2008) were seen to accompany elevated levels of cytosolic Ca^{2+} concentration ($[Ca^{2+}]_c$) and mitochondrial Ca^{2+} overload in *Jam-A* (*Junctional adhesion molecule A*) null mice where PMCA4 activity is known to be significantly decreased (Aravindan *et al.*, 2012).

The mechanism by which the absence of PMCA4 or its reduced activity results in loss of sperm motility or asthenozoospermia (AZ) is unknown. Also, studies of PMCA4's interacting partners in sperm are limited and only just beginning: in murine sperm PMCA4b was detected to be in association with Ca^{2+}/CaM-dependent serine kinase (CASK) to which it binds preferentially at relatively low $[Ca^{2+}]_c$, via its PDZ (PSD-95/Dlg/ZO1) ligand (Aravindan *et al.*, 2012). In human sperm, although PMCA4 has not yet been localized, its presence has been inferred from studies in which its inhibitor was demonstrated to cause a decrease in sperm motility (Williams and Ford, 2003; Jimenez-Gonazalez *et al.*, 2004; Peralta-Arias *et al.*, 2015).

In attempting to elucidate the underlying mechanism of the loss of sperm motility in the absence of PMCA4 activity, it is of interest to determine PMCA4's interacting partners in sperm. In neuronal and endothelial cells, PMCA4 is known to negatively regulate nNOS (Schuh *et al.*, 2001) and eNOS (Holton *et al.*, 2010). These constitutive NOSs are present in mammalian sperm (Herrero *et al.*, 1996; O'Bryan *et al.*, 1998) where they are responsible for the synthesis of NO which is required for a variety of sperm functional activities including hyperactivated motility, capacitation and the acrosome reaction (Herrero and Gagnon, 2001). Importantly, they are rapidly activated by Ca^{2+} (Knowles and Moncada, 1994), and elevated levels of NO result in AZ and male infertility (Ramya *et al.*, 2011). In this study we ask whether or not PMCA4 in human sperm dynamically interacts with nNOS and eNOS whose encoding gene, *eNOS*, is known to harbor a single nucleotide polymorphism (SNP) that is associated with AZ and male infertility (Buldreghini *et al.*, 2010).

Interestingly, PMCA4a was recently shown to be expressed and secreted in the bovine (Brandenburger *et al.*, 2011) and murine epididymides where it is present on epididymosomes and where it is involved in epididymal sperm maturation (Patel *et al.*, 2013). We have also demonstrated that PMCA4a is expressed in the female tract where it is associated with uterosomes and oviductosomes from which it can be delivered to sperm during capacitation (AL-Dossary *et al.*, 2013). These findings raise the possibility that PMCA4 may also be expressed in prostasomes which have been shown to recruit sperm to deliver Ca^{2+} signaling tools (Aalberts *et al.*, 2013).

Based on the above, we hypothesized that prostasomes carry PMCA4 and its interacting partners in their cargo that they deliver to sperm. Our results reveal the co-localization of PMCA4 with eNOS and nNOS at the posterior head/neck junction of the sperm and show that PMCA4 is physically associated with each, preferentially during periods of elevated $[Ca^{2+}]_c$ when down-regulation of NOS activity would prevent elevated levels of NO and its resulting toxicity and loss of sperm motility. Thus we provide insights into the mechanism underlying the loss of motility and fertility in PMCA4's absence in sperm. Importantly, we show that PMCA4 and its interacting partners are present in prostasomes which are able to deliver these fertility-modulating proteins to the sperm *in vitro*.

Materials and Methods

Human samples and reagents

The use of human material was approved by the University of Delaware Human Subject Review Board. Fresh semen samples were obtained from patients attempting IVF/ICSI at the Reproductive Associates of Delaware (RAD) Laboratory (Christiana Hospital in Newark, DE, USA). Laboratory personnel assessed samples using standard World Health Organization (WHO) criteria (WHO, 2010) which included sperm concentration, percentage motility and motility grade, prior to donating them to our lab with an anonymous identification number. Informed consent was obtained from all subjects providing samples. All enzymes and chemicals were purchased from Fisher Scientific Co. (Malvern, PA, USA), Sigma (St. Louis, MO, USA) or Invitrogen (Carlsbad, CA, USA), unless otherwise specified.

Antibodies

Affinity purified goat polyclonal pan-PMCA4 antibody (Y20, sc 22080; recognizes both 4a and 4b isoforms) raised against the N-terminus of the rat protein was purchased from Santa Cruz Biotechnology (Santa Cruz, CA, USA), along with rabbit polyclonal anti-eNOS antibody (C20 or NOS3) which maps at the C-terminal end of NOS3 in humans, and with rabbit polyclonal anti-nNOS antibody (NOS1 or R20). Anti-rat CASK/Ln2 mouse monoclonal antibody (#75–000), which cross-reacts with the human protein, was obtained from UC Davis/NINDS/NIMH NeuroMab Facility (Davis, CA, USA). Secondary antibodies were purchased from Life Technologies, Santa Cruz Biotechnology, or Molecular Probes Inc. (Eugene, OR, USA). These antibodies were used in western blots, co-immunoprecipitation (Co-IP) assays, indirect immunofluorescence (IF) and fluorescence resonance energy transfer (FRET) studies, all of which demonstrated their specificity in detecting these proteins in humans.

Isolation of sperm, seminal plasma and prostasomes

Semen samples selected for the study were those with a progressive motility rate of ≥50%. Sperm were separated from liquefied samples by centrifugation at 500*g* for 20 min and the seminal plasma collected. The seminal plasma was clarified following the removal of cellular debris after centrifugation at 16 000*g* for 20 min at 4°C. Prostasomes were isolated from the clarified seminal plasma by a process similar to that previously described (Caballero *et al.*, 2013). Briefly, using a Beckman Optima L-70 centrifuge with a Ti60 rotor, clarified seminal plasma was subjected to ultracentrifugation at 120 000*g* for 2 h at 4°C. Both insoluble (pellet) and soluble (supernatant) fractions were collected and used in Western analysis while purified unfractionated seminal plasma was used for Co-IP assays. Proteins from the soluble fraction were precipitated with three volumes of acetone and recovered in sample buffer for western blotting, as described (Zhang and Martin-DeLeon, 2003; Patel *et al.*, 2013), along with the pellet (containing the prostasomes) that was also re-suspended in the sample buffer.

Sperm were studied under physiological states where $[Ca^{2+}]_c$ varied. Comparisons were made for uncapacitated and capacitated, or uncapacitated and Ca^{2+} ionophore-treated (acrosome-reacted) sperm which had the highest level of $[Ca^{2+}]_c$, while uncapacitated had the lowest. Sperm collected in 100–200 μl of capacitating medium, HTF (Human tubal fluid; InVitroCare, Frederick, MD, USA) were either incubated at 37°C for 2 h (capacitated) or immediately processed (uncapacitated). For Ca^{2+}-ionophore treatment, sperm were placed in 100 μl HTF medium containing 1 μM A23187 calcium ionophore and incubated at 37°C for 65 min.

Downloaded from https://academic.oup.com/molehr/article/21/11/832/2459813 by guest on 24 April 2024

Localization of PMCA4, eNOS, nNOS and CASK on human sperm membrane, using indirect immunofluorescence

Sperm samples, isolated as described above, were washed three times with phosphate-buffered saline (PBS), and recovered by centrifugation for 20 min each at 500*g*. They were then fixed with 1.5% paraformaldehyde for 1 h at room temperature (or stored overnight in paraformaldehyde at 4°C), washed (3×, 20 min) with PBS and then permeabilized with 0.1% Triton X-100 for 10 min at room temperature. After washing, cells were blocked with 2% bovine serum albumin in PBS for 30 min and then incubated with primary antibodies: anti-PMCA4 (Y20), anti-eNOS (C20), anti-nNOS (R20) each at a dilution of 1:50, and/or anti-CASK (1:500) at 4°C overnight. The controls contained rabbit or goat immunoglobulin (Ig)G where appropriate. The secondary antibodies were Alexa Fluor 555-conjugated donkey anti-goat IgG (Molecular Probes, Eugene Oregon) for PMCA4 and Alexa Fluor 488-conjugated goat anti-rabbit IgG for eNOS and nNOS, all diluted 1:200. After 30 min incubation in the dark, cells were washed (3×, 20 min) with PBS. They were then re-suspended in ~45 μl PBS and smears made on slides to which ~10 μl of proLong Gold with 4′,6-Diamidino-2-phenylindole (DAPI) was added for counter-staining. Slides were examined using a Zeiss LSM 780 confocal microscope (Carl Zeiss, Inc., Gottingen, Germany) using a plan-Apochromatic 63× or 40× oil objective.

To determine if PMCA4 is present on the inner acrosomal membrane (IAM), sperm treated with Ca^{2+} ionophore [where typically >90% of the cells are acrosome-reacted (Deng *et al.*, 1999)] were immunostained with anti-PMCA4 antibodies, while its presence over the acrosome was probed with fluorescein isothiocyanate (FITC)-conjugated peanut agglutinin (PNA) lectin which stains the acrosomal matrix. Thus after treatment with the anti-PMCA4 secondary antibodies, uncapacitated sperm were counter-stained with 10 μg/ml PNA-FITC as described (Modelski *et al.*, 2014). If the red PMCA4 signal is present on the acrosome beyond background level, it is expected to merge with the green FITC staining to give a yellow coloration, while in its absence the green is unchanged.

Co-localization and FRET via acceptor photobleaching

To co-localize the proteins sperm were fixed, permeabilized and immunostained as described above with a few modifications; namely, the primary antibodies were added in two pairs: anti-PMCA4 and anti-eNOS, and anti-PMCA4 and anti-nNOS. Secondary antibodies were also added in sets corresponding to the primary antibodies. Slides were visualized using a Zeiss LSM 780 confocal microscope and analyzed using ZEN software (Carl Zeiss, Inc., Gottingen, Germany).

FRET was used to study molecular scale interactions between two sets of proteins: PMCA4/eNOS and PMCA4/nNOS. In this technique an excited fluorophore (a donor) transfers its excited energy to a light-absorbing molecule (an acceptor) if the molecules are closer than ~100 Å. FRET efficiencies were evaluated using the Acceptor Photobleaching approach described by Bragdon *et al.* (2009, 2010). For this, a donor fluorophore (green label, Alexa Fluor 488, which excites at 488 nm) was used to tag eNOS and nNOS and an acceptor fluorophore (red, Alexa Fluor 555, which excites at 561 nm) was used for PMCA4. The Forster distance (R0, the distance at which energy transfer efficiency is 50% of the maximum possible for a particular donor-acceptor) for Alexa Fluor 488 and Alexa Fluor 555 is known to be 70 Å (Life Technologies). With the occurrence of FRET the donor encounters a quenching of its fluorescence due to the energy transfer to the acceptor. However after photobleaching of the acceptor, donor fluorescence is unquenched. The difference between the average fluorescence intensities of the donor after and before bleaching divided by the average post-bleach intensity provides a direct assessment of the FRET efficiency.

To obtain the data, lasers were used to excite the fluorophores and a region of interest (ROI) encompassing a sperm was selected and five initial images of the donor fluorophore were taken. Following the bleaching event, which consisted of 40 iterations of the laser, to ensure that the acceptor was fully bleached and that there would be maximal enhancement of the donor, 15 more images were captured. Thus, there were a total of 20 images/cell. These high resolution and high magnification images were collected, using confocal microscopy (with a Zeiss LSM 780 confocal microscope; Carl Zeiss, Inc., Gottingen, Germany) with a plan-Apochromatic 63× oil objective and the FRET module.

Using Image J (U.S. National Institute of Health, Bethesda, MD, USA), the area of the ROI was calculated and normalized for the intensity values for pre- and post-bleach. Also, the background fluorescence was calculated using Image J and subtracted from the pre- and post-intensity values. There were a total of eight treatment groups analyzed: (i) four for PMCA4/eNOS, two of which were uncapacitated (UNCAP), pre- and post-bleaching and two were capacitated (CAP), pre- and post-bleaching; and (ii) four for PMCA4/nNOS in the categories described for PMCA4/eNOS.

Co-IP assays with sperm and seminal plasma proteins

Co-IP assays of sperm proteins were similar to those previously described from our laboratory (Modelski *et al.*, 2014). Briefly, PureProteome Protein G magnetic beads (Millipore Corp, Billerica, MA, USA) were washed twice in PBS with 0.1% Tween 20 and recovered by centrifugation at 2500*g* for 5 min. They were then re-suspended in 100 μl of PBS with 2 μg of anti-PMCA4 antibodies (anti-eNOS or anti-nNOS antibodies) for 2 h at 4°C, while the control received the same concentration of appropriate IgG (goat for PMCA4 and rabbit for the NOSs). After incubation, the beads were centrifuged at 2500*g*, and the supernatant removed prior to washing them with PBS. The beads were then re-suspended in 150–200 μg of sperm proteins [obtained from a lysate in RIPA buffer (Cell Signaling, Danvers, MA, USA) supplemented with protease inhibitor (PI)]. In the case of clarified seminal plasma, a volume containing 300–500 μg of proteins was diluted with RIPA buffer containing PI before adding to the beads. This sperm protein suspension was then brought to a final volume of 500 μl with the addition of immunoprecipitation buffer (25 mM Tris, 150 mM NaCl, pH 7.2) with PI (or 250 μl for clarified seminal plasma). Following incubation in the protein suspensions for overnight at 4°C, the beads were recovered by centrifugation and all but 20 μl of the fluid removed. Loading dye (5 μl of a 5× solution) was added to the fluid and the beads were re-suspended.

The bead suspension was then boiled for 5 min and the reduced protein eluate analyzed by sodium dodecyl sulfate polyacrylamide gel electrophoresis (SDS-PAGE, 8% gel) and electro-transferred to nitrocellulose membranes. Membranes were probed using rabbit anti-eNOS primary antibody (1:250) or rabbit anti-nNOS primary antibody (1:500) and detected with alkaline phosphatase-conjugated anti-rabbit secondary antibody, or in some cases detected with multilink secondary antibody (1:5000) from BioGenex. Visualization was performed with the WesternBreeze Chemiluminescent immunodetection kit (Invitrogen).

In the reciprocal Co-IP either nNOS or eNOS antibody (2 μg) was used in the immunoprecipitation step, while the membranes were probed with goat anti-PMCA4 antibody (1:100). Detection occurred with donkey anti-goat biotin-conjugated secondary antibodies (Jackson Laboratory, West Grove, PA, USA) diluted 1:5000, followed by SA-HRP (Streptavidin-horse-radish peroxidase, Jackson Laboratory, diluted 1:5000) incubation, and bands were visualized using HRP (EMD Millipore Corporation). At least three experiments were performed for each of the partner pairs.

Downloaded from https://academic.oup.com/molehr/article/21/11/832/2459813 by guest on 24 April 2024

SDS-PAGE and western blot analysis

Sperm and prostasome samples were homogenized with either homogenization buffer (62.5 mM Tris–HCl, 10% glycerol, 1% SDS) or 1× RIPA buffer [~180 μl, containing PI], using a mortar and pestle. Protein concentrations in the lysates and seminal plasma were determined using the Pierce bicinchoninic acid protein assay Kit (Thermo Scientific, Rockford, IL, USA), according to the manufacturer's protocol. Samples for electrophoresis were diluted in 5× Laemmli sample buffer and incubated for 5 min at 99°C. Twenty to 60 μg of proteins were loaded per lane on 10% polyacrylamide gels and transferred onto a nitrocellulose membrane (Amersham Biosciences).

Blots were blocked for 1 h at room temperature and incubated in primary antibodies: anti-eNOS (1:250), anti-nNOS (1:500), anti-PMCA4 (1: 100) or anti-CASK (1:1000) overnight at 4°C. Non-specific binding of antibody was removed using washes (5×) of TBST (20 mM Tris, pH 8.0, containing 150 mM NaCl and 0.5% Tween 20) before incubation in the alkaline phosphatase (AP)-conjugated anti-rabbit IgG (Invitrogen, diluted 1:2000) or AP-conjugated anti-goat IgG (Sigma-Aldrich, diluted 1:30 000) or AP-conjugated anti-mouse IgG (Invitrogen 1:2000) for 1 h at 4°C. The membrane was again washed (6×, 15 min) using TBST before chemiluminescence was detected by using the ECL kit (Bio-Rad, Hercules, CA, USA).

In vitro sperm uptake of PMCA4, eNOS and nNOS from seminal plasma, as detected via co-incubation and flow cytometric analysis

Freshly collected sperm were isolated from semen as described above and co-incubated in the seminal plasma isolated from the semen sample, for 6 h at 37°C. Following incubation sperm were centrifuged at 500*g* for 15 min, the supernatant was removed and the sperm were fixed with 4% paraformaldehyde overnight. After fixation the cells were permeabilized, blocked, and treated with anti-PMCA4, anti-eNOS, or anti-nNOS primary antibody (1:50) followed by treatment with secondary antibody (chicken anti-goat Alexa Fluor 488 for PMCA4 or goat anti-rabbit 488 for the NOSs), as described above. Cells were subjected to flow cytometric analysis, using a FACSCalibur unit (Becton Dickinson, San Diego, CA) equipped with an argon laser with excitation at 488 nm. The control untreated sperm were aliquots isolated from the same individual as the treated sample and processed similarly, without co-incubation with seminal plasma.

Statistical Analysis

A one-way ANOVA followed by a *post hoc* Tukey Kramer [SAS (SAS Institute, Cary, NC, USA)] analysis was performed to determine significance among the eight treatment groups in the FRET analysis. For FRET efficiency, Student's two-tailed *t*-test [SAS (SAS Institute)] was used to calculate significant differences between treatment pairs. Significant differences were recorded for *P*-values <0.05.

Results

IF and confocal microscopy revealed that PMCA4 is localized over the head, the neck and midpiece, and the proximal principal piece (Fig. 1a). The staining varied: it was most intense on the neck/midpiece junction and least intense over the acrosome where it was found in only 5% of the cells analyzed (Table I). The absent/low intensity red PMCA4 staining on the plasma membrane over the acrosome is revealed by the unaltered green staining of the acrosomal matrix (Fig. 1d). However, following the acrosome reaction, PMCA4 staining on the IAM was seen (Fig. 1e) in >50% of 40 sperm analyzed from two subjects. eNOS was found to be localized predominantly on the posterior head and the neck/midpiece junction, where the staining was most intense (Table I, Fig. 1b). nNOS appeared to be more abundant than eNOS and to be more widely distributed as it was seen over the anterior (acrosome) and posterior head, the neck/midpiece junction, and the principal piece (Fig. 1c). The absence of staining in the negative controls (Fig. 1a–c,E) confirmed the specificity of the antibodies used. Unlike the other proteins, CASK is absent from the head and is localized to the midpiece and the proximal principal piece (Fig. 1f).

Staining for the localization of each protein and the co-localization experiment was done on capacitated sperm where the $[Ca^{2+}]_c$ is elevated. Figure 2a shows that PMCA4 and eNOS co-localize at the base of the head near the midpiece and the principal piece, identified as a yellow signal where the red and green images merged. The most intense yellow staining was seen at the base of the head near the neck. For PMCA4 and nNOS, the most intense area of co-localization is also seen in the base of the head and the proximal principal piece (Fig. 2b). Thus the co-localizations overlapped at the base of the head near the neck region and occurred in >92% of the cells with the eNOS-PMCA4 pair and 62% of those analyzed for nNOS-PMCA4. It should be noted that while the staining in Figs 1 and 2 was typical, there was a wide spectrum of variability within an individual, with some sperm having little or no staining in each of the regions identified (Fig. 2c and d). For nNOS some sperm had very heavy deposits of the staining on the anterior head (Fig. 2d, arrowed).

Co-IP assays showed that anti-PMCA4 antibodies were able to immunoprecipitate eNOS in proteins from Ca^{2+} ionophore-treated or acrosome-reacted sperm, but only marginally so in uncapacitated sperm (Fig. 3A). The 140 kDa eNOS is seen in the total sperm protein used as a positive control, but missing in the IgG control. This finding suggests that eNOS and PMCA4 are in close association after Ca^{2+} ionophore treatment when calcium levels are elevated. Similarly, Fig. 3B shows that the 155 kDa nNOS could also be co-immunoprecipitated with anti-PMCA4 antibodies after Ca^{2+} ionophore treatment, but to a much lower extent in the untreated, again showing a close interaction at elevated $[Ca^{2+}]_c$.

In Fig. 4A and B post-bleaching fluorescence intensities were shown to increase for PMCA4-eNOS and PMCA4-nNOS pairs, indicating that FRET had occurred for both. Significant differences in the intensities were seen between CAP and UNCAP samples at both pre-bleaching ($P < 0.05$) and post-bleaching ($P < 0.001$) stages for eNOS and $P < 0.01$ and $P < 0.0001$ for nNOS, suggesting more molecules of the NOSs are recruited at a close distance to PMCA4 during capacitating, compared with uncapacitating, conditions where $[Ca^{2+}]_c$ is elevated. This is consistent with the Co-IP data, where more interaction is seen at elevated $[Ca^{2+}]_c$ after treatment with the ionophore.

When FRET efficiencies were calculated, the average ranged from 12 to 30% (Fig. 4C). These values represent the fraction of the donor (eNOS or nNOS) molecules that exhibit FRET. The highest efficiency (30%) was seen for the PMCA4-nNOS pair under non-capacitating conditions. This efficiency was significantly ($P < 0.001$) higher than the 12% seen for the UNCAP PMCA4-eNOS pair, which was significantly ($P < 0.01$) lower than the 22% rate seen for CAP PMCA4-eNOS pair. For CAP sperm, the 26% efficiency rate for the PMCA4-nNOS pair was more than double the 12% rate for the UNCAP PMCA4-eNOS pair, a significant ($P < 0.01$) difference, but not significantly different from the 30% PMCA4-nNOS UNCAP pair. There was also a significant ($P < 0.05$) difference between the rates for PMCA4-eNOS CAP and PMCA4-nNOS UNCAP.

Downloaded from https://academic.oup.com/molehr/article/21/11/832/2459813 by guest on 24 April 2024

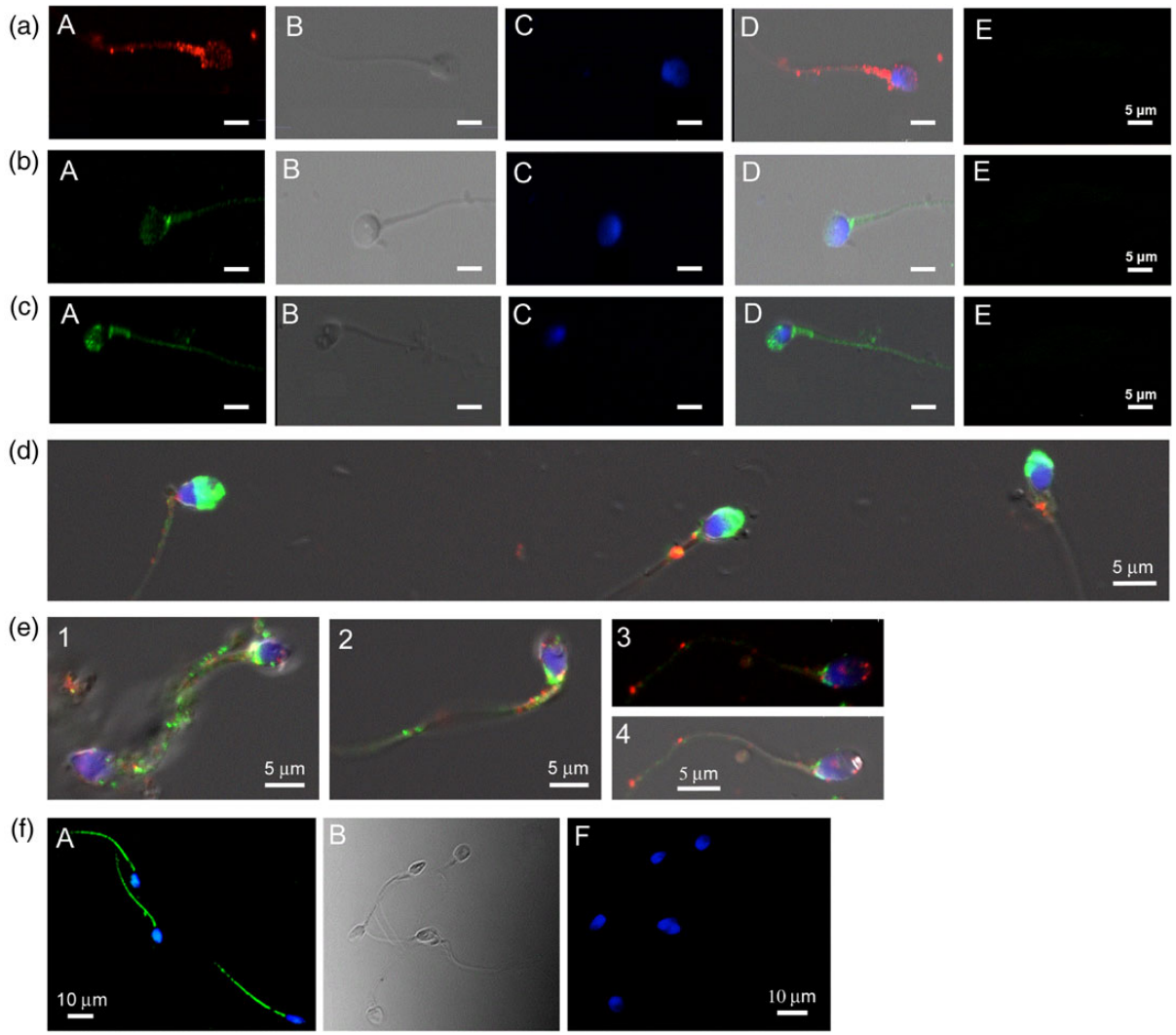

Figure 1 Indirect immunofluorescence of human sperm shows that PMCA4 and the NOSs are localized on the head and flagellum. (**a**) Plasma membrane Ca^{2+}-ATPase 4 (PMCA4), red) is seen over the acrosome, midpiece and proximal principal piece, (**b**) endothelial nitric oxide synthase (eNOS, green) on the neck and posterior head, and (**c**) neuronal NOS (nNOS, green) is more broadly distributed on the head and flagellum. IgG negative control is seen in (E). (A) represents the primary antibody staining, (B) is the differential interference contrast (DIC) image, (C) is 4′,6-Diamidino-2-phenylindole (DAPI staining) while (D) is the merged image showing the base of the head and the neck to have the most intense staining in the areas of overlap for the three proteins. (**d**) Acrosome-intact sperm stained for PMCA4 and the acrosomal matrix. The green fluorescein isothiocyanate (FITC)-conjugated peanut agglutinin staining on the acrosome is unaltered in the absence, or low intensity, of the red PMCA4 signal on the plasma membrane over the acrosome. The necks and midpieces have the red signal. (**e**) Acrosome-reacted sperm stained for PMCA4 and eNOS show eNOS at the posterior head/neck junction and the red signal on the inner acrosomal membrane and the neck of 1–4 in merged images, as seen in (D) of (a)–(c). The sperm in (e-4) is seen in transmitted light in (e-3). (**f**) Ca^{2+}/CaM-dependent serine kinase (CASK) is present on the midpiece and the proximal principal piece and absent from the sperm head (A), after staining with anti-CASK antibodies. The immunoglobulin (IgG) negative control is seen in (F) where the head is stained with DAPI, (B) is the DIC image of (F) showing the presence of the tails.

Prostasomes isolated from the seminal plasma of three men were probed in Western analysis to detect the presence of PMCA4 and its interacting partners, eNOS and nNOS, as well as CASK which was shown earlier to interact with PMCA4b more strongly in UNCAP than CAP murine sperm proteins (Aravindan *et al.*, 2012). In Fig. 5A–D, using sperm proteins as a positive control, it is shown that human prostasomes carry the ~130 kDa PMCA4, along with its interacting partners, eNOS (140 kDa), nNOS (155 KDa), as well as CASK (~60 kDa). For CASK, mouse sperm proteins were used as a control and showed both the insoluble (~100 kDa) and the soluble (60 kDa) isoforms of CASK. Only the soluble isoform, which is known to interact with the PDZ ligand of PMCA4, was seen in the human prostasome samples. In Fig. 5C and D, proteins were precipitated from the supernatant recovered from ultracentrifugation of the clarified seminal plasma and gave no bands when subjected to Western analysis, indicating that the proteins in the seminal plasma are carried in prostasomes.

Downloaded from https://academic.oup.com/molehr/article/21/11/832/2459813 by guest on 24 April 2024

Table I Immunofluorescence expression of plasma membrane Ca^{2+}-ATPase 4 (PMCA4), nitric oxide synthases (NOSs), and Ca^{2+}/CaM-dependent serine kinase (CASK) in human sperm with ≥50% motility.

Protein	Cells Analyzed (*n*)	% Cells Stained	% of cells stained in different regions				
			ACR	Post. Head	Neck	Midpiece	PPP
PMCA4	49	98	5	82	92	75	85
eNOS	38	74	10	76	100	68	70
nNOS	42	100	72	68	94	100	96
CASK	36	96	–	–	–	100	100

Sperm were analyzed from four men.
ACR, acrosome; Post., posterior; PPP, proximal principal piece; eNOS, endothelial NOS; nNOS, neuronal NOS.

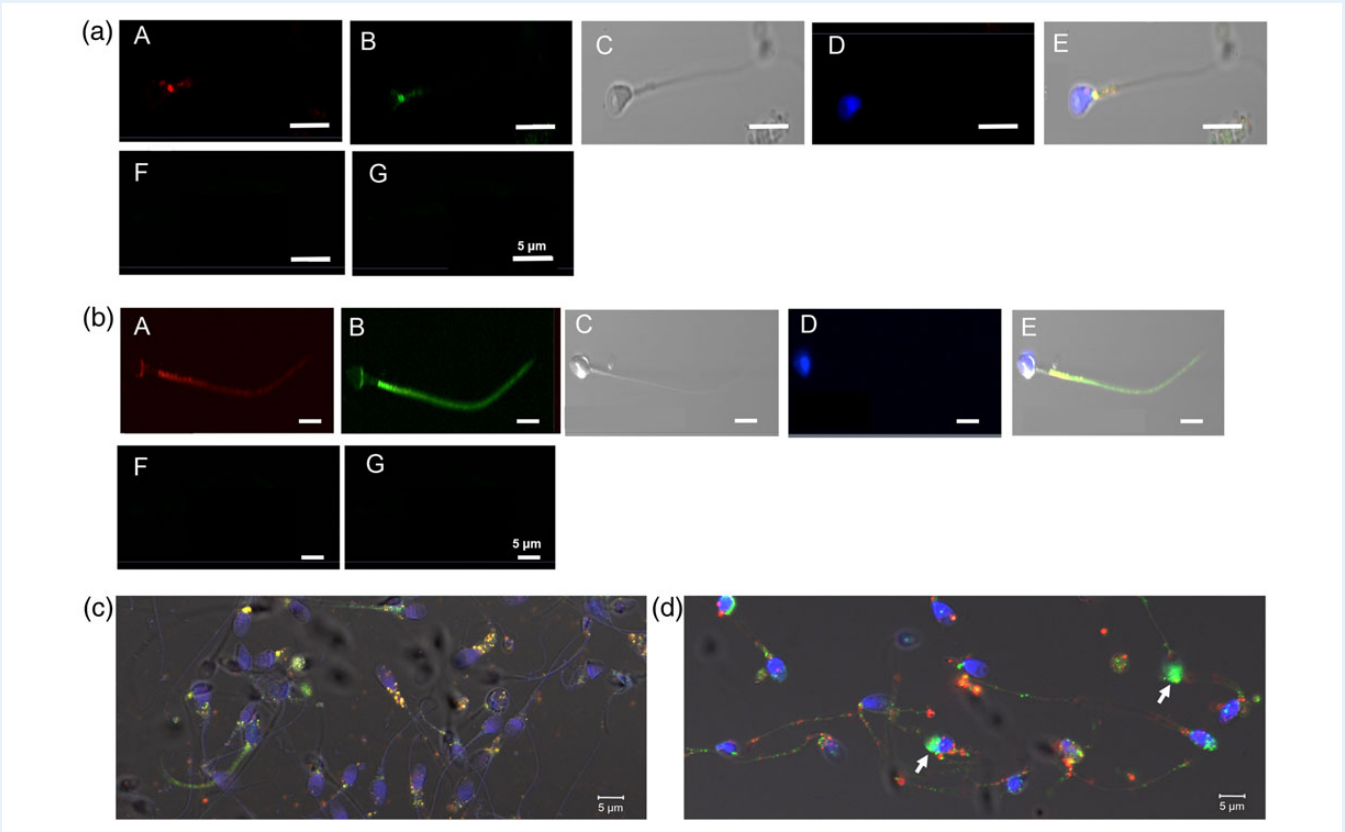

Figure 2 PMCA4 co-localizes with eNOS and nNOS. Co-localization of (**a**) PMCA4 and eNOS, where (A) is PMCA4 and (B) is eNOS; (**b**) PMCA4 and nNOS, where (A) is PMCA4 and (B) is nNOS is shown. (C) is the DIC image, (D) is the DAPI staining, and (E) is the merged images of the two proteins identified as a yellow signal. Negative controls, using goat serum and rabbit IgG, are seen in (F) and (G). Bar = 5 µm. Merged images of groups of cells showing co-localization of eNOS and PMCA4 are seen in (**c**), and for nNOS and PMCA4 in (**d**) where heavy deposits of staining of the anterior head are marked (white arrow).

To investigate if the interactions of PMCA4 and its partners seen in sperm proteins also occur in prostasomes, Co-IP assays were performed on the proteins in the seminal plasma. Figure 6A shows the Western for the Co-IP for PMCA4 and eNOS, indicating that PMCA4 and its interacting partners are intimately associated in prostasomes in the seminal plasma. This finding was confirmed by reciprocal Co-IPs (Fig. 6B). Figure 6C shows a similar close association for PMCA4 and nNOS in prostasomes, with confirmation from the reciprocal Co-IPs (Fig. 6D). Thus the protein complexes seen in sperm also exist in the prostasomes.

Following co-incubation of sperm with their seminal plasma, prostasomes were shown to be capable of delivering PMCA4 and its interacting partners, eNOS and nNOS, to sperm (Fig. 7). An increase of ~2.3-fold in PMCA4 fluorescence intensity in sperm incubated with the seminal plasma compared with control was observed for one individual

Downloaded from https://academic.oup.com/molehr/article/21/11/832/2459813 by guest on 24 April 2024

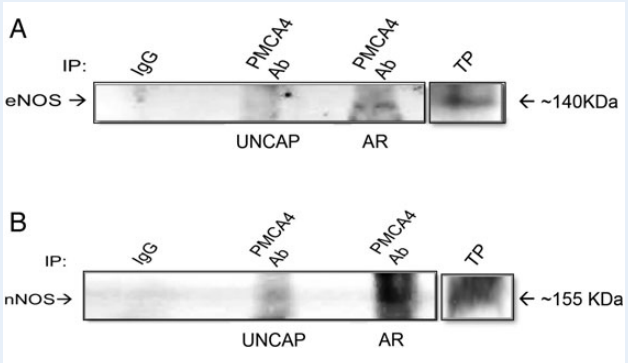

Figure 3 Co-immunoprecipitation assays show a close association of PMCA4 and the NOSs. Increased binding of PMCA4 and the NOSs is seen in proteins from acrosome-reacted (AR), compared with that in uncapacitated (UNCAP), human sperm. In (**A**) the 140 kDa eNOS and (**B**) the 155 kDa nNOS band are detected after co-immunoprecipitation. Goat IgG was used as a negative control and shows the specificity of the Co-IP. Total protein (TP) was used as a positive control.

(Fig. 7A) and a 5-fold increase for another after the same co-incubation period (data not shown) in duplicate experiments performed. Increases in intensity of ~8-fold for eNOS (Fig. 7B) and 4-fold for nNOS (Fig. 7C) were detected compared with the untreated controls. Therefore our findings are consistent with the notion that PMCA4, eNOS and nNOS are among the proteins delivered by prostasomes to sperm following their recruitment *in vivo* in the female.

Discussion

Localization of PMCA4 and its interacting partners

PMCA4 is known to be the most efficient Ca^{2+} efflux pump in murine sperm (Wennemuth *et al.*, 2003). This is most likely the case for human sperm, based on the 84% amino acid identity of the protein in mouse and human (NCBI Blast). While PMCA4's localization in human sperm has only been speculated (Jimenez-Gonzalez *et al.*, 2004) to date, we show for the first time that it localizes on the head, neck, midpiece and proximal principal piece (Fig. 1) of human sperm. Importantly, PMCA4 was found to be present on the IAM where it was recently found to be localized in the mouse (AL-Dossary *et al.*, 2015). This localization is physiologically relevant with respect to Ca^{2+} clearance after the elevated influx that accompanies the acrosome reaction.

PMCA4's localization showed both inter- and intra-individual variation. This heterogeneity in ejaculated sperm may be due to differential storage periods in the epididymis where they are likely to acquire the protein to augment their testicular endowment, based on reports for other mammals (Brandenburger *et al.*, 2011; Patel *et al.*, 2013).

The localization of PMCA4 on the midpiece and neck region is interesting since these are regions of lipid rafts (Cross, 2004), where it is known to exist in somatic cells (Sepúlveda *et al.*, 2006) as well as in murine sperm (Aravindan *et al.*, 2012). As a signaling molecule, PMCA4's localization in lipid rafts of human sperm is of physiological significance. During capacitation lipid rafts are known to concentrate interacting molecules to initiate signaling cascades, amid the changes that occur in the lipid composition and redistribution within the sperm plasma membrane (Cross, 2004). PMCA4's localization with respect to other calcium tools is also interesting. Its localization at the neck where a calcium store has been reported (Costello *et al.*, 2009) and on the proximal principal piece where the Ca^{2+} influx channel, CATSPER, resides (Tamburrino *et al.*, 2014) shows the spatially regulated nature of calcium signaling.

Similar to PMCA4, CASK was localized for the first time in human sperm and was shown to be on the midpiece and proximal principal piece. It is absent from the head, as reported in the mouse (Aravindan *et al.*, 2012). Interestingly, localization of eNOS overlapped with that of PMCA4 in the neck, midpiece and proximal principal piece (Fig. 2), where lipid raft microdomains exist (Cross, 2004). Furthermore, staining of eNOS appeared specifically on the equatorial regions of the head as well as the neck, midpiece, and principal piece (Fig. 1). This finding is only in partial agreement with the report by O'Bryan *et al.* (1998) which did not detect eNOS on the flagellum, but concurs with that of Salvolini *et al.* (2012). Our results showing that nNOS is found on the acrosome and flagellum in human sperm (Fig. 1) and exists in greater abundance than eNOS are also in agreement with those of Salvolini *et al.* (2012) and are consistent with the finding of Herrero *et al.* (1996). Both of these reports also detected cell-to-cell variation in protein expression, as seen in the present study. This is likely to arise, similarly to that for PMCA4, from epididymal acquisition over different storage periods, since eNOS is expressed in the human epididymis (Zini *et al.*, 1996) and both NOSs are present in the murine epididymal fluid which can deliver them to sperm (our unpublished data).

As PMCA4, eNOS and nNOS were found in overlapping regions when they were probed for individually, it was not surprising to detect their co-localization (Fig. 2). This occurred on the posterior head near the neck and the proximal principal piece, where they are likely to be in a cluster to serve dynamic functional roles. Since the principal piece is known to play a role in motility (Tamburrino *et al.*, 2014), it can be postulated that the proteins are assembled in these regions in order to regulate motility in human sperm (Schlingmann *et al.*, 2007). Furthermore, the presence of the proteins on the posterior head suggests that they are also important for fertilization (Toshimori *et al.*, 2011).

PMCA4 interacts preferentially with eNOS and nNOS at elevated $[Ca^{2+}]_c$

Ca^{2+} uptake in sperm has been shown to be biphasic with the lower influx associated with capacitation, while the second and more elevated peak mediates acrosomal exocytosis (Fraser, 1987; de Lamirande *et al.*, 1997). Thus for AR sperm, the $[Ca^{2+}]_c$ >CAP $[Ca^{2+}]_c$ >UNCAP $[Ca^{2+}]_c$. In this study basal $[Ca^{2+}]_c$ in uncapacitated sperm was compared with either that in capacitated or Ca^{2+} ionophore-induced AR sperm to investigate functional interaction. The reciprocal Co-IP data revealed that for both PMCA4-eNOS and PMCA4-nNOS pairs, interactions occurred predominantly in AR sperm compared with UNCAP sperm (Fig. 3), reflecting an association that is Ca^{2+}-dependent.

Since co-immunoprecipitated proteins might not be directly interacting we performed FRET assays to determine direct interactions of PMCA4 and the NOSs and to ask whether or not the interaction varied with $[Ca^{2+}]_c$. eNOS is known to interact with PMCA4 at the catalytic domain on the larger cytosolic loop (Holton *et al.*, 2010), while

Downloaded from https://academic.oup.com/molehr/article/21/11/832/2459813 by guest on 24 April 2024

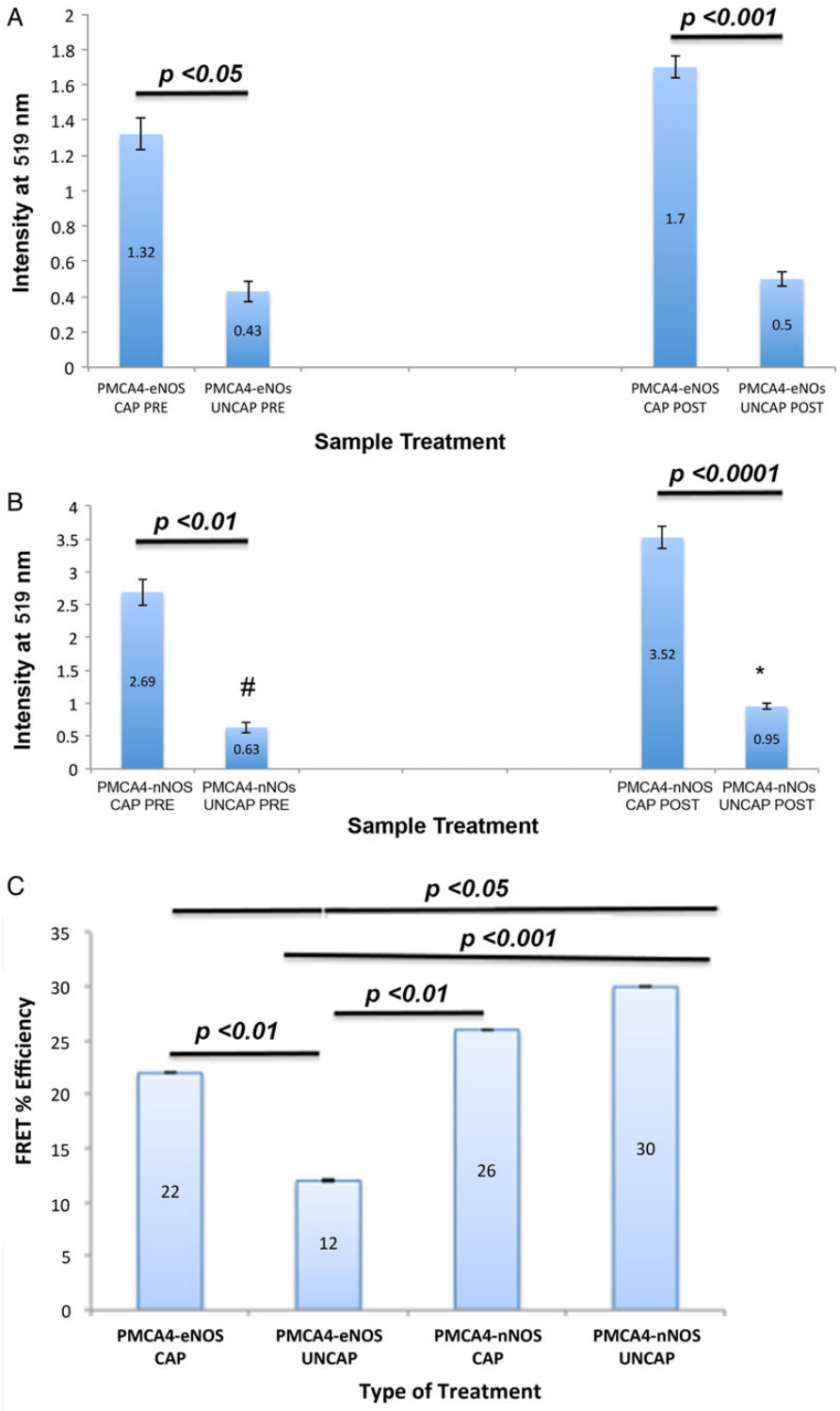

Figure 4 Data analysis reveals that FRET occurs for PMCA4 and the NOSs. Representative graphs of the average pre-bleaching (PRE) and post-bleaching (POST) fluorescence intensities in capacitated (CAP) and uncapacitated (UNCAP) human sperm for eNOS (**A**) and nNOS (**B**). Post-bleaching intensities of both increased, indicating that FRET had occurred. Intensities were significantly higher for CAP versus UNCAP sperm both PRE- and POST-bleaching for eNOS-PMCA4 ($P < 0.05$; $P < 0.001$) and for nNOS-PMCA4 ($P < 0.01$; $P < 0.0001$) interactions. (**C**) The average % FRET efficiencies (the fractions of donor molecules, eNOS and nNOS, that exhibit FRET) varied for the four treatment groups, being highest for nNOS interactions. Significant differences in FRET efficiencies were found for PMCA4-eNOS CAP versus UNCAP ($P < 0.01$), for both PMCA4-nNOS and PMCA4-eNOS UNCAP ($P < 0.001$), for PMCA4-nNOS CAP versus PMCA4-eNOS UNCAP ($P < 0.01$), and PMCA4-eNOS CAP versus PMCA4-nNOS UNCAP ($P < 0.05$). A total of 10–11 cells and 20 images per cell were analyzed for each group. Error bars represent standard error (SEM). Data were analyzed by one-way ANOVA followed by a *post hoc* Tukey Kramer analysis and the Students two-tailed *t-test*.

Downloaded from https://academic.oup.com/molehr/article/21/11/832/2459813 by guest on 24 April 2024

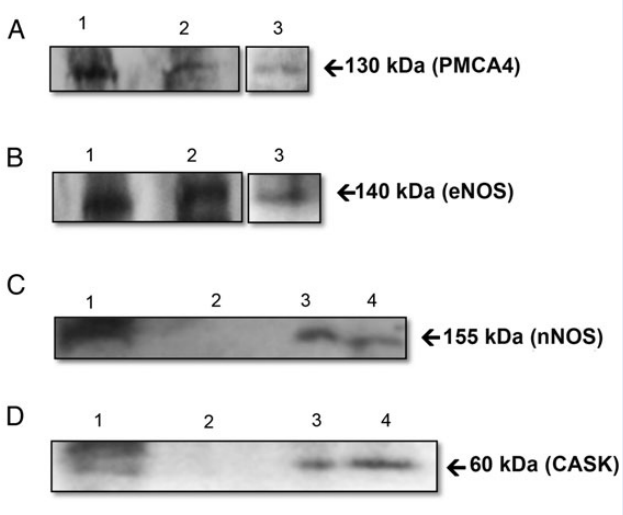

Figure 5 PMCA4 and its interacting partners are present in human prostasomes. (**A**) shows PMCA4 protein bands, ~124–133 KDa, representing the 4a and 4b isoforms from two individuals (lanes 1 and 2). (**B**) shows eNOS (140 KDa) in prostasomes from two individuals (lanes 1 and 2). Lanes 3 in (A) and (B) show human sperm proteins used as a control. (**C**) shows nNOS (155 KDa) in prostasomes (lane 3), clarified seminal plasma (SP) (lane 4), and human sperm protein (lane 1); while lane 2 shows its absence in the supernatant recovered after ultracentrifugation of SP for isolation of the prostasomes. (**D**) shows the presence of CASK in mouse sperm, used as a positive control (lane 1), prostasomes (lane 3), clarified seminal plasma (SP) (lane 4), and its absence in the supernatant following ultracentrifugation of SP (lane 2).

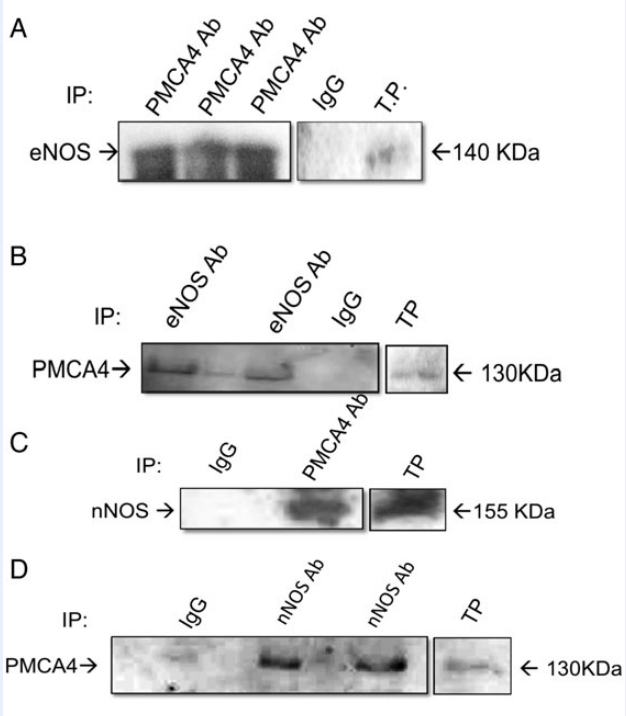

Figure 6 Reciprocal Co-IPs reveal that PMCA4 and the NOSs are closely associated in prostasomes in human seminal plasma. Anti-PMCA4 antibody was used to co-immunoprecipitate eNOS (140 KDa) (**A**) and nNOS (155 KDa) (**C**), with goat IgG and total sperm protein used as negative and positive control, respectively. Anti-eNOS and anti-nNOS antibodies were used to co-immunoprecipitate PMCA4 (~130 KDa) (**B** and **D**). Rabbit IgG and sperm proteins were, respectively, used as the negative and positive control.

nNOS has a PDZ domain via which it interacts with the PDZ ligand at the C-terminus of PMCA4 (Schuh *et al.*, 2001). Thus both can interact with PMCA4 simultaneously, as we have detected in Fig. 3 [While PMCA4 is known to interact in other ternary complexes in somatic cells (Schuh *et al.*, 2001; Holton *et al.*, 2010), this is the first such complex which involves both constitutive NOSs]. In this vein, Fig. 4 shows that there are significantly higher donor fluorescence intensities in capacitated samples compared with uncapacitated ones, following the acceptor bleaching event for both PMCA4-eNOS and PCMA4-nNOS pairs. These data indicate that at high $[Ca^{2+}]_c$ more of the NOS molecules are in close proximity (i.e. within 10 nm) of PMCA4, confirming the preferential physical association detected under this condition with the Co-IP assays.

Since the interaction of PMCA4 with the NOSs in somatic cells results in their down-regulation (Schuh *et al.*, 2001; Holton *et al.*, 2010), a similar interaction in sperm is likely to also inhibit eNOS and nNOS at a time when their heightened activity is favored by elevated $[Ca^{2+}]_c$. It should be noted that calcium ionophore (A23187, used to generate AR sperm) is a potent activator of constitutive NOSs (Donnelly *et al.*, 1997). Thus when $[Ca^{2+}]_c$ is globally high, tethering the NOSs to activated PMCA4 would ensure that they would be in a local environment of relatively low $[Ca^{2+}]_c$ as Ca^{2+} is ejected into the extracellular space. The resulting down-regulation of the NOSs in this locale is of physiological significance, since NO (in elevated levels) is known to be an inhibitor of sperm motion (Nobunaga *et al.*, 1996). Increased NO levels would generate elevated peroxynitrite levels after binding to superoxide. As peroxynitrite is a highly reactive oxygen species (ROS) and is cytotoxic at high levels, the interaction of PMCA4 and the NOSs prevents toxic levels of ROS which are known to lead to lipid peroxidation. Sperm, with membranes which are enriched in polyunsaturated fatty acids, are vulnerable to lipid peroxidation which is a key mechanism for loss of motility (Hellstrom *et al.*, 1994; Aitken *et al.*, 2014). Thus it is likely that in murine sperm with targeted disruption of *Pmca4*, the AZ results from NO toxicity in PMCA4's absence.

With respect to FRET efficiencies the NOSs behaved differently. The PMCA4-eNOS pair displayed a significantly higher FRET efficiency at elevated $[Ca^{2+}]_c$ in capacitated sperm, compared with that at basal $[Ca^{2+}]_c$. The greater number of molecules interacting at elevated $[Ca^{2+}]_c$ would inhibit the heightened activity of eNOS which occurs under this condition. However, PMCA4-nNOS samples for which uncapacitated sperm had the highest FRET efficiency (30%) had significantly higher efficiencies than the PMCA4-eNOS pairs, for both capacitated and uncapacitated sperm. Thus the data suggest that at both elevated and basal $[Ca^{2+}]_c$ more nNOS molecules, unlike those for eNOS, are inhibited by PMCA4. This is likely due to the greater abundance of nNOS and also its existence in both an insoluble and a soluble form (Matsumoto *et al.*, 1993). Since human nNOS binds to PMCA4 at basal $[Ca^{2+}]_c$ in uncapacitated sperm when PMCA4 is also known to bind CASK in murine sperm (Aravindan *et al.*, 2012), human sperm PMCA4 might be interacting with both nNOS and CASK simultaneously via its PDZ

Downloaded from https://academic.oup.com/molehr/article/21/11/832/2459813 by guest on 24 April 2024

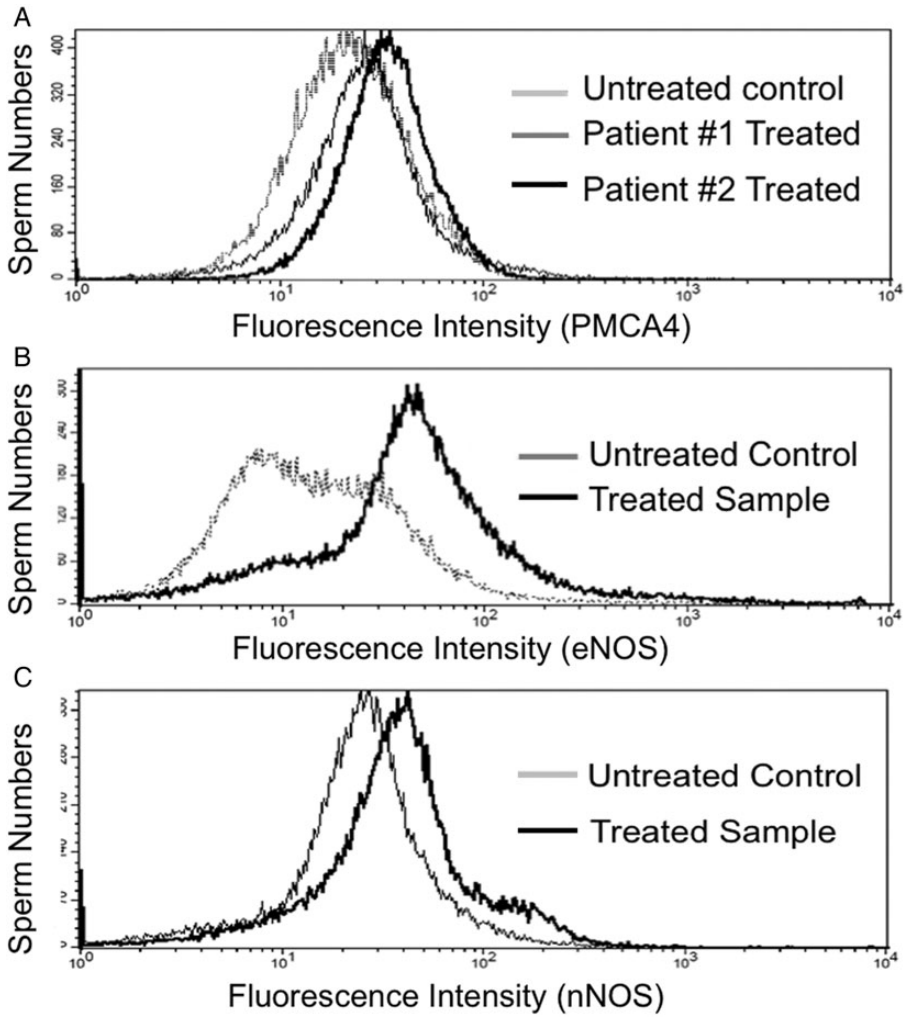

Figure 7 PMCA4 and the NOSs are delivered to human sperm by prostasomes in the seminal plasma. Quantitative immunofluorescence, detected by flow cytometry, demonstrates the acquisition of PMCA4 (**A**), eNOS (**B**) and nNOS (**C**) after co-incubation of human sperm and seminal plasma from the same individuals at 37°C for 6 h. Fluorescence intensity increased 2.3-fold for PMCA4 uptake in the treated sample versus the control, as seen from the peak shift towards the right. For eNOS (B) and nNOS (C) the respective increases were 8.0- and 4-fold versus the untreated control. A total of 50 000 sperm were analyzed for each sample.

ligand. This is not only probable, but highly likely, since PMCA4 functions as a dimer (Di Leva *et al.*, 2008) and one monomer could bind to CASK and the other to nNOS.

CASK, PMCA4 and the NOSs are present in prostasomes where PMCA4 and the NOSs are in a complex which can be delivered to sperm *in vitro*

Since prostasomes are known to carry Ca^{2+} signaling tools (Park *et al.*, 2011) we investigated if they also carry PMCA4, eNOS, nNOS and CASK. Our results in Fig. 5 show that all are present in prostasomes, which are membrane vesicles residing in the seminal plasma. These vesicles are known to deliver a variety of proteins to the sperm surface, including those responsible for sperm motility (Aalberts *et al.*, 2013). While PMCA4 is a transmembrane protein, CASK, eNOS, and nNOS are membrane-associated proteins. It should be noted that CASK and nNOS (Fig. 5C and D) and also PMCA4 and eNOS (data not shown) were shown to be present in prostasomes but absent from the supernatant after ultracentrifugation of the clarified seminal plasma. Thus in Co-IP assays of seminal plasma we show that similar to sperm, eNOS and nNOS in prostasomes are in intimate association with PMCA4 (Fig. 6). Since the 60 kDa CASK which is known to interact via its PDZ domain (Funke *et al.*, 2005) was detected in prostasomes (Fig. 5D), it is likely to be associated with a population of PMCA4 molecules via their PDZ ligands, as occurs in murine sperm proteins (Aravindan *et al.*, 2012).

Mammalian spermatozoa are known to undergo post-testicular maturation by interacting with the epididymal luminal fluid and prostatic fluid, so the presence of these proteins in prostasomes underscores their importance in sperm physiology (Aalberts *et al.*, 2013; Sullivan and Saez, 2013). Prostasomes are known to fuse with sperm to deliver their

Downloaded from https://academic.oup.com/molehr/article/21/11/832/2459813 by guest on 24 April 2024

cargo (Park et al., 2011; Aalberts et al., 2013) and it has already been discovered that prostasomes are capable of delivering to human sperm members of the calcium signaling toolkit in response to progesterone (Park et al., 2011; Aalberts et al., 2013). In Fig. 7 we show that PMCA4, eNOS and nNOS can be delivered to sperm *in vitro*. This may likely be in the form of a complex, based on our Co-IP results and a recent report for epididymosomes (Martin-DeLeon, 2015). Thus prostasomes not only transport Ca^{2+} influx molecules, but also molecules for Ca^{2+} efflux and those involved in NO signaling.

Conclusions

This study identifies for the first time the localization of PMCA4, a major Ca^{2+} efflux pump, and CASK in human sperm. It shows that nNOS is more abundant than eNOS in human sperm and, along with PMCA4 and CASK, is present in prostasomes which can deliver these proteins to sperm. Although both NOSs interact with PMCA4 dynamically and preferentially at elevated $[Ca^{2+}]_c$, significantly more molecules of nNOS than eNOS are involved. The results support the hypothesis that at high $[Ca^{2+}]_c$ PMCA4 simultaneously interacts with eNOS and nNOS in human sperm in a novel ternary inhibitory complex to negatively regulate NO production to prevent oxidative stress. The latter is likely to be responsible for the loss of motility and infertility in *Pmca4* null sperm. Our findings suggest that screening men with AZ might reveal *PMCA4*, *nNOS and eNOS* mutations, as already seen for *eNOS* (Buldreghini et al., 2010). Besides improving diagnosis of AZ, the work also points to a therapeutic strategy for a subset of AZ patients in the IVF clinic. Due to the diffusible nature of NO, it can be readily removed or added to sperm *in vitro*, depending on whether levels are elevated or reduced, both of which are associated with AZ (Ramya et al., 2012).

Acknowledgements

We are indebted to the Reproductive Associates of Delaware for access to the sperm samples used in this study. Without their support this work would not be possible. Thanks are due to Michael Moore and Dr Jeffrey Caplan for assistance with confocal microscopy and the FRET studies, and to Dr Rolands Aravindan for preparing the image with the immunofluorescence of CASK. We appreciate also the assistance with statistics obtained from Dr John MacDonald.

Authors' roles

R.E.A. and P.A.M.-D. designed the research and analyzed the data, R.E.A. performed most of the experiments, D.S.G. carried out the FACS analysis, and R.E.A. and P.A.M.-D. wrote the paper. The work was submitted by R.E.A. in partial fulfillment of the requirements for the Master's degree.

Funding

This work was supported by NIH-RO3HD073523 and NIH NCRR 2P20 RR015588-09 to P.A.M-D.

Conflict of interest

None declared.

References

Aalberts M, Sostaric E, Wubbolts R, Wauben MW, Nolte-t Hoen EN, Gadella BM, Stout TA, Stoorvogel W. Spermatozoa recruit prostasomes in response to capacitation induction. *Biochim Biophys Acta* 2013; **1834**:2326–2335.

Aitken RJ, Smith TB, Jobling MS, Baker MA, De Iuliis GN. Oxidative stress and male reproductive health. *Asian J Androl* 2014;**16**:31–38.

AL-Dossary AA, Strehler EE, Martin-DeLeon PA. Expression and secretion of plasma membrane Ca^{2+}-ATPase 4a (PMCA4a) during murine estrus: association with oviductal exosomes and uptake in sperm. *PLoS One* 2013;**8**:e80181.

AL-Dossary AA, Bathala P, Caplan JL, Martin-DeLeon PA. Oviductosome-sperm membrane interaction in cargo delivery: detection of fusion and underlying molecular players using 3D super-resolution structured illumination microscopy (SR-SIM). *J Biol Chem* 2015;**290**:17710–17723.

Aravindan GR, Fomin VP, Naik UP, Modelski MJ, Naik MU, Galileo DS, Duncan RL, Martin-DeLeon PA. CASK interacts with PMCA4b and JAM-A on the mouse sperm flagellum to regulate Ca^{2+} homeostasis and motility. *J Cell Physiol* 2012;**227**:3138–3150.

Bragdon B, Thinakaran S, Bonor J, Underhill TM, Petersen NO, Nohe A. FRET reveals novel protein-receptor interaction of bone morphogenetic proteins receptors and adaptor protein 2 at the cell surface. *Biophys J* 2009;**97**:1428–1435.

Bragdon B, Thinakaran S, Moseychuk O, King D, Young K, Litchfield DW, Petersen NO, Nohe A. Casein kinase 2 beta-subunit is a regulator of bone morphogenetic protein 2 signaling. *Biophys J* 2010;**99**:897–904.

Brandenburger T, Strehler EE, Filoteo AG, Caride AJ, Aumuller G, Post H, Schwarz A, Wilhelm B. Switch of PMCA4 splice variants in bovine epididymis results in altered isoform expression during functional sperm maturation. *J Biol Chem* 2011;**286**:7938–7946.

Buldreghini E, Mahfouz RZ, Vignini A, Mazzanti L, Riccardo-Lamonica G, Lenzi A, Agarwal A, Ballerica G. Single nucleotide polymorphism (SNP) of the endothelial nitric oxide synthase (eNOS) gene (Glu298Asp Variant) in infertile men with asthenozoospermia. *J Androl* 2010; **31**:482–488.

Caballero JN, Frenette G, Belleannee C, Sullivan R. CD9-positive microvesicles mediate the transfer of molecules to Bovine Spermatozoa during epididymal maturation. *PLoS One* 2013;**8**:e65364.

Caride AJ, Filoteo AG, Penniston JT, Strehler EE. The plasma membrane Ca^{2+} pump isoform 4a differs from isoform 4b in the mechanism of calmodulin binding and activation kinetics: implications for Ca^{2+} signaling. *J Biol Chem* 2007;**282**:25640–25648.

Costello S, Michelangeli F, Nash K, Lefievre L, Morris J, Machado-Oliveira G, Barratt C, Kirkman-Brown J, Publicover S. Ca^{2+}-stores in sperm: their identities and functions. *Reproduction* 2009;**138**:425–437.

Cross NL. Reorganization of lipid rafts during capacitation of human sperm. *Biol Reprod* 2004;**71**:1367–1373.

de Lamirande E, Leclerc P, Gagnon C. Capacitation as a regulatory event that primes spermatozoa for the acrosome reaction and fertilization. *Mol Hum Reprod* 1997;**3**:175–194.

DeMarco SJ, Strehler EE. Plasma membrane Ca^{2+}-ATPase isoforms 2b and 4b interact promiscuously and selectively with members of the membrane-associated guanylate kinase family of PDZ (PSD95/Dlg/ZO-1) domain-containing proteins. *J Biol Chem* 2001;**276**:21594–21600.

Deng X, Czymmek K, Martin-DeLeon PA. Biochemical maturation of Spam1 (PH-20) during epididymal transit of mouse sperm involves modifications of *N*-linked oligosaccharides. *Mol Reprod Dev* 1999;**52**:196–206.

Di Leva F, Domi T, Fedrizzi L, Lim D, Carafoli E. The plasma membrane Ca^{2+} ATPase of animal cells: structure, function and regulation. *Arch Biochem Biophys* 2008;**476**:65–74.

Downloaded from https://academic.oup.com/molehr/article/21/11/832/2459813 by guest on 24 April 2024

Donnelly ET, Lewis SEM, Thompson W, Chakravarthy U. Sperm nitric oxide and motility: the effects of nitric oxide synthase stimulation and inhibition. *Mol Hum Reprod* 1997;**3**:755–762.

Fraser LR. Minimum and maximum extracellular Ca^{2+} requirements during mouse sperm capacitation and fertilization. *J Reprod Fertil* 1987;**81**:77–89.

Funke L, Dakoji S, Bredt DS. Membrane-associated guanylate kinases regulate adhesion and plasticity at cell junctions. *Annu Rev Biochem* 2005; **74**:219–245.

Hellstrom WJG, Bell M, Wang R, Sikka SC. Effect of sodium nitroprusside on sperm motility, viability, and lipid peroxidation. *Fertil Steril* 1994; **61**:1117–1122.

Herrero MB, Gagnon C. Nitric oxide. A novel mediator of sperm function. *J Androl* 2001;**22**:349–356.

Herrero MB, Perez Martinez S, Viggiano JM, Polak JM, Gimeno MF. Localization by indirect immunofluorescence of nitric oxide synthase in mouse and human spermatozoa. *Reprod Fertil Dev* 1996;**8**:931–934.

Holton M, Mohamed TM, Oceandy D, Wang W, Lamas S, Emerson M, Neyses L, Armesilla AL. Endothelial nitric oxide synthase activity is inhibited by the plasma membrane calcium ATPase in human endothelial cells. *Cardiovasc Res* 2010;**87**:440–448.

Jimenez-Gonzalez C, Michelangeli F, Harper CV, Barratt CL, Publicover SJ. Calcium signalling in human spermatozoa: a specialized 'toolkit' of channels, transporters and stores. *Hum Reprod Update* 2004;**3**:253–267.

Knowles RG, Moncada S. Nitric oxide synthases in mammals. *Biochem J* 1994; **298**:249–258.

Martin-DeLeon PA. Epididymosomes: transfer of fertility-modulating proteins to the sperm surface. *Asian J Androl* 2015;**17**:720–725.

Matsumoto T, Nakane M, Pollock JS, Kuk JE, Förstermann U. A correlation between soluble brain nitric oxide synthase and NADPH-diaphorase activity is only seen after exposure of the tissue to fixative. *Neurosci Lett* 1993;**155**:61–64.

Modelski MJ, Menlah G, Wang Y, Dash S, Wu K, Galileo DS, Martin-DeLeon PA. Hyaluronidase 2: a novel germ cell hyaluronidase with epididymal expression and functional roles in mammalian sperm. *Biol Reprod* 2014;**91**:1–11.

Nobunaga T, Tokugawa Y, Hashimoto K, Kubota Y, Sawai K, Kimura T, Shimoya K, Takemura M, Matsuzaki N, Azma C *et al.* Elevated nitric oxide concentration in the seminal plasma of infertile males: nitric oxide inhibits motility. *Am J Reprod Immunol* 1996;**36**:193–197.

O'Bryan MK, Zini A, Cheng CY, Schlegel PN. Human sperm endothelial nitric oxide synthase expression: correlation with sperm motility. *Fertil Steril* 1998;**70**:1143–1147.

Okunade GW, Miller ML, Pyne GJ, Sutliff RL, O'Connor KT, Neumann JC, Andringa A, Miller DA, Prasad V, Doetschman T *et al.* Targeted ablation of plasma membrane Ca^{2+}-ATPase (PMCA) 1 and 4 indicates a major housekeeping function for PMCA1 and a critical role in hyperactivated sperm motility and male fertility for PMCA4. *J Biol Chem* 2004; **279**:33742–33750.

Park KH, Kim BJ, Kang J, Nam TS, Lim JM, Kim HT, Park JK, Kim YG, Chae SW, Kim UH. Ca^{2+} signaling tools acquired from prostasomes are required for progesterone-induced sperm motility. *Sci Signal* 2011;**4**:173.

Patel R, Al-Dossary AA, Stabley DL, Barone C, Galileo DS, Strehler EE, Martin-DeLeon PA. Plasma membrane Ca^{2+}-ATPase 4 in murine epididymis: secretion of splice variants in the luminal fluid and a role in sperm maturation. *Biol Reprod* 2013;**89**:1–11.

Peralta-Arias RD, Vivenes CY, Camejo MI, Pinero S, Proverbio T, Martınez E, Marın R, Proverbio F. ATPases, ion exchangers and human sperm motility. *Reproduction* 2015;**149**:475–484.

Ramya T, Man Mohan M, Devabrata S, Nandan D, Sandeep M. Altered levels of seminal nitric oxide, nitric oxide synthase, and enzymatic antioxidants and their association with sperm function in infertile subjects. *Fertil Steril* 2011;**95**:135–140.

Salvolini E, Buldreghini E, Lucarini G, Vignini A, Di Primio R, Balercia G. Nitric oxide synthase and tyrosine nitration in idiopathic asthenozoospermia: an immunohistochemical study. *Fertil Steril* 2012;**97**:554–560.

Schlingmann K, Michaut MA, McElwee JL, Wolff CA, Travis AJ, Turner RM. Calmodulin and CaMKII in the sperm principal piece: evidence for a motility-related calcium/calmodulin pathway. *J Androl* 2007; **28**:706–716.

Schuh K, Uldrijan A, Telkamp M, Rothlein N, Neyses L. The plasma membrane calmodulin-dependent calcium pump: a major regulator of nitric oxide synthase I. *J Cell Biol* 2001;**273**:18693–18696.

Schuh K, Cartwright EJ, Jankevics E, Bundschu K, Liebermann J, Williams JC, Armesilla AL, Emerson M, Oceandy D, Knobeloch KP *et al.* Plasma membrane Ca^{2+} ATPase 4 is required for sperm motility and male fertility. *J Biol Chem* 2004;**279**:28220–28226.

Sepúlveda MR, Berrocal-Carrillo M, Gasset M, Mata AM. The plasma membrane Ca^{2+}-ATPase isoform 4 is localized in lipid rafts of cerebellum synaptic plasma membranes. *J Biol Chem* 2006;**281**:447–453.

Shao M, Ghosh A, Cooke VG, Naik UP, Martin-DeLeon PA. JAM-A is present in mammalian spermatozoa where it is essential for normal motility. *Dev Biol* 2008;**313**:246–255.

Sullivan R, Saez F. Epididymosomes, prostasomes and liposomes; their role in mammalian male reproductive physiology. *Reproduction* 2013; **146**:R21–R35.

Tamburrino L, Marchiani S, Minetti F, Forti G, Muratori M, Baldi E. The CatSper calcium channel in human sperm: relation with motility and involvement in progesterone-induced acrosome reaction. *Hum Reprod* 2014;**29**:418–428.

Toshimori K. Dynamics of the mammalian sperm membrane modification leading to fertilization: a cytological study. *J Electron Microsc* 2011;**60** Suppl 1:S31–S42. doi: 10.1093/jmicro/dfr036.

Wennemuth G, Babcock DF, Hille B. Calcium clearance mechanisms of mouse sperm. *J Gen Physiol* 2003;**122**:115–128.

Williams KM, Ford WC. Effects of Ca^{2+}-ATPase inhibitors on the intracellular calcium activity and motility of human spermatozoa. *Int J Androl* 2003;**26**:366–375.

World Health Organization. *Laboratory Manual for the Examination and Processing of Human Semen*. Geneva: WHO Press, 2010.

Zhang H, Martin-DeLeon PA. Mouse epididymal Spam1 (PH-20) is released in the luminal fluid with its lipid anchor. *J Androl* 2003;**24**:51–58.

Zini A, O'Bryan MK, Magid MS, Schlegel PN. Immunohistochemical localization of endothelial nitric oxide synthase in human testis, epididymis, and vas deferens suggests a possible role for nitric oxide in spermatogenesis, sperm maturation, and programmed cell death. *Biol Reprod* 1996;**55**:935–939.

Downloaded from https://academic.oup.com/molehr/article/21/11/832/2459813 by guest on 24 April 2024